International Journal of Mass Spectrometry and Ion Physics, 22 (1976) 221–235

FIELD IONIZATION ENERGY SPECTRA OF MOLECULES*

A. J. JASON AND A. C. PARR
Department of Physics and Astronomy, The University of Alabama, Alabama 35486 (U.S.A.)
(First received 22 August 1975; in final form 22 December 1975)

ABSTRACT

Considerations for determination of the partition of internal energy in ions formed by field ionization are discussed in terms of the distribution of ion energies. Experimental high-resolution energy spectra for the molecular ions produced by field ionization of toluene, cycloheptatriene, phenol, hydrogen and carbon monoxide are shown and discussed. In particular it is concluded that the range of internal energies can be of the order of several electron volts. Implications of the observations for rate predictions are discussed.

INTRODUCTION

The phenomenon of ionization of atoms or molecules by their interaction with a high electric field near a metallic surface, i.e. field ionization, has been useful for investigation of surfaces on a microscopic scale [1] and for use as an ion source in the mass-spectrometric study of organic molecules [2]. These separate applications have been investigated as nearly independent subjects so that workers in each application have developed phenomenological viewpoints appropriate to their task. The varying viewpoints provide simplifying assumptions which ignore some major aspect of the field ionization process. Usually, either the structure of the substance being ionized or the structure of the emitter surface is de-emphasized; in both cases the basic energetics of the field ionization process is often ignored.

A basic theory of field ionization and fragmentation rates must include each of these three factors: molecular structure, surface structure, and energies and

* Work supported in part by Grant AFOSR 74-2726 and in part by the Research Grants Committee of The University of Alabama.

accessibility of final states. This latter factor forms the primary concern of this paper and is important since it contributes to the consolidation of surface and molecular viewpoints. Observation of the contributions of final molecular and metal states is accomplished by high-resolution energy analysis of field ionization products. The energy spectra thus obtained along with kinetic considerations and the condition of conservation of energy provide a spectroscopy involving the contribution of molecular final states. Data are presented to show the field ionization spectrum of H_2, a dissociative system, and of CO which does not detectably dissociate. These spectra are related to the molecular energy structure. Further data are presented for three organic molecules; toluene, cycloheptatriene, and phenol, and their spectra similarly interpreted. Finally, the implications of these results are discussed, together with some possible applications to field ionization mass spectrometry.

FIELD IONIZATION ENERGY SPECTROSCOPY

The rate of ionization by impact methods such as photoionization or electron bombardment are understood in terms of the system energetics; the net energy of the system is conserved with rearrangement of the energy (and hence often the geometry) in a manner consonant with the internal constraints of the system and the system energy levels. One of the methods of exploring the partition of energy among the system levels is to monitor the relative reaction rate as a function of energy input via the bombarding particle. In particular the minimum electron or photon energy for detectable ionization or fragmentation (i.e. the appearance potential) is an important parameter.

Field ionization takes place with no energy input (excluding polarization energy by the high electric field) to the neutral molecule; the gain in energy of the molecular electron which tunnels into the metal is exactly offset by a decrease in potential energy of the ion formed. The decrease in potential energy then becomes a "deficit" in kinetic energy after acceleration through the field. It has been shown by considering available states in the emitter material that if I is the energy necessary to remove an electron from an atom or molecule leaving the ion in a particular state, the maximum kinetic energy, E_c, at which that ion can be observed is $E_c = V_0 - I + \varphi$ [3]. Here V_0 is the emitter potential, referenced to the ion detector potential (usually ground), φ the emitter work function and E_c is called the critical energy. It is convenient to define a quantity ΔE known as the energy-deficit, $\Delta E = V_0 - E$, where E is the ion kinetic energy at the ion detector. The critical energy-deficit is then $\Delta E_c = I - \varphi$. In practice φ is replaced by an instrumental quantity which is independent of the emitter work function. We have verified experimentally this linear relationship between I and the critical energy-deficit, as have other workers [4]. The energy spectra of field-emitted ions

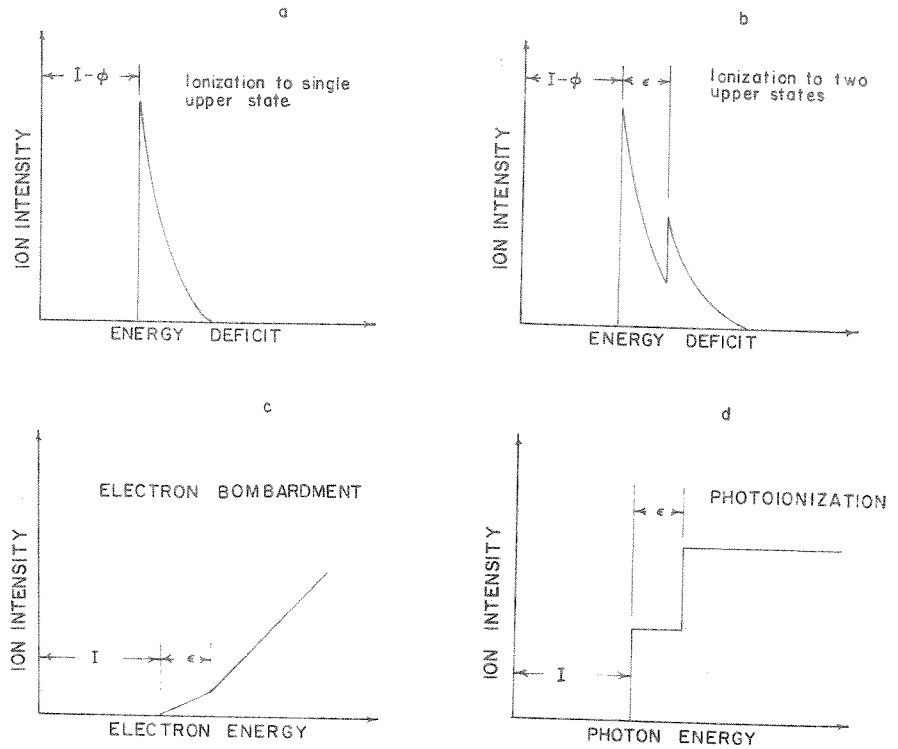

Fig. 1. Comparisons of threshold ionization characteristics for field ionization, electron impact ionization and photoionization. The abscissas are the appropriate energetic parameter to describe the molecular energy balance, i.e., energy-deficit, electron energy or photon energy in arbitrary units. The ordinates are ion intensity in arbitrary units. (a) Idealized energy distributions of ions from field ionization. An abrupt onset at energy $I-\phi$ is followed by intensity decreasing at a rate given by dynamic considerations. Transition to a single ionic state is assumed. (b) Idealized energy distribution of ions from field ionization as in (a) but with an additional ionic electronic state at an energy ε above the ground state. (c) The threshold law for electron impact is approximately a linear increase in intensity with energy. The accessibility of a second state at an energy ε above the ground state would cause a break in the curve and a change in the slope. (d) The threshold law for photoionization is approximately a step function. In the case of two accessible states the ion intensities add to give the step structure indicated.

can be predicted to provide many of the features contained in scans of ionization rate versus particle energy obtained from bombardment experiments. This correspondence is illustrated in Fig. 1. which portrays schematically the presumed role of upper states in the spectra. Figure 1(a) gives the general features of a field ionization energy distribution for ionization to an upper state. The general form of this peak as depicted has been experimentally verified [5, 6]. A sharp rise at onset is featured with a gradual tail at higher energy-deficits as a result of diminished ionization probability for ions originating farther from the surface.

If a single excited state exists at an energy ε above the ionic ground state and the transition probability to both states are similar, a distribution as shown in Fig. 1(b) would be expected; transitions to the excited state would produce a superimposed second peak with onset at $\Delta E = I+\varepsilon-\varphi$. Depending upon the value of ε and the inherent width of the two peaks in Fig. 1(b), structure may be evident in the energy distributions. Figures 1(c) and 1(d) demonstrate a presumed correspondence of the field ionization spectra to the ion-appearance spectra obtained by electron bombardment and photoionization respectively. The correspondence is determined by a change in the total ionization probability as the energetics become favorable for transitions from the ground state of the neutral molecule to the accessible states of the ion. Because of these expected similarities between ionization by bombardment and field ionization we suggest that investigation of the energy spectra of field ionization products can provide information as to the partition of internal energy among final ionic states.

Field ionization energy spectra have been explored with high resolution for inorganic samples. Inghram and Gomer [7, 8] performed the first field ionization energy analyses. They noted that the mass peaks were broadened and discovered, among other things, that the peak-widths increased with increasing electric field. Young and Müller [9] and Müller and Bahadur [10, 11] were the first to obtain high-resolution energy distributions for inert gases and hydrogen. They clearly demonstrated the existence of the predicted critical energy-deficit and discussed other features such as the distribution width. Jason et al. [12], using hydrogen as the sample gas, found further detail in the spectra arising from interaction of the gas with the surface. They also found spectra of the fragment peak, H^+, which are interpretable in terms of the dissociation kinetics. The dissociation of hydrogen during field ionization was later studied in greater detail by Hanson et al. [13], and Hanson [14] who carefully examined the dissociation kinetics. The energy spectrum of an associated reaction, the formation of H_3^+, has also been published [12]. Aside from these investigations, most high-resolution studies of field ionization energy spectra have been done with a view toward explaining phenomena encountered in field ion microscopy.

In view of the above discussion we consider investigation of field ionization energy spectra important for the purpose of obtaining a fundamental theory of field ionization mass spectra in the same way that consideration of the energetics of electron bombardment ionization contributes to the understanding of mass spectra produced by electron bombardment.

EXPERIMENTAL

Energy analyses were performed using a 60°, 12-in. radius-of-curvature, magnetic analyzer. The practical energy resolution obtainable with this instrument is ca. 1 part in 10,000. The instrument features a bakeable ultra-high-vacuum

system, dual gas inlet, and temperature-controlled source (from 450 °C. to liquid-helium temperatures). An electron bombardment ion source is included in the instrument for use as a conventional mass spectrometer. Ions in this experiment originated from a small area of a single tungsten tip. After passing through an aperture which subtends an angle of ca. 5° (i.e. ions emitted within a solid angle of ca. 4×10^{-3} steradian centered about the tip pass through the aperture), the ion beam is focused on to the entrance slit of the magnetic analyzer by an electric quadrupole doublet lens [15]. A retarding energy analyzer [6] is situated between the quadrupole lens and the analyzer slit. It is used for absolute calibration of the energy-deficit spectra. The magnetic analyzer focuses the beam onto a 20-stage particle detector capable of monitoring individual events or an integrated current. Since the ion intensities obtained using single tip emitters are low (i.e. on the order of 10–500 events s^{-1}), a multiscaler is used to acquire digital data. The address of the multiscaler is proportional to a slow negative sweep voltage (of magnitude equal to the total energy scan) applied to the emitter in addition to the accelerating potential, V_0. Hence this varying voltage sweeps over the ion energy distribution and at any time equals ΔE, the energy-deficit to within a determinable additive constant. The multiscaler directly plots the ion intensity versus energy-deficit. After many such sweeps statistically significant data concerning the differential energy distribution are obtained.

The samples used in this experiment were research grade materials and the organic samples were vacuum distilled before introduction to the field ionization source. Electron bombardment analysis was used to check sample purity. Background pressure in the instrument was of the order of 10^{-8} torr or lower and experiments were performed at room temperature. Ion energies for the organic samples were ca. 1 kV with an applied field of ca. 10^8 V cm^{-1}. At the fields used, ionization far from the surface was not appreciable and fragmentation was negligible. Single tip emitters were used in these studies rather than multiple emitters because it was desired to eliminate any effects which would result from emission from more than one emitter crystal plane. Use of a single tip emitter also provides a definite field and lower ion energies with consequent higher resolution.

RESULTS AND DISCUSSION

The existence of an onset energy-deficit is depicted graphically in Fig. 2 in which a plot of the number of ion counts of the parent ion for a phenol sample versus a differential voltage applied to the accelerating potential is given. The abscissa is hence related to the energy-deficit, ΔE, by an additive quantity. Data were taken by obtaining a field ionization signal and accumulating over repetitive 20-V energy-deficit sweeps at constant magnetic field to obtain the peak on the

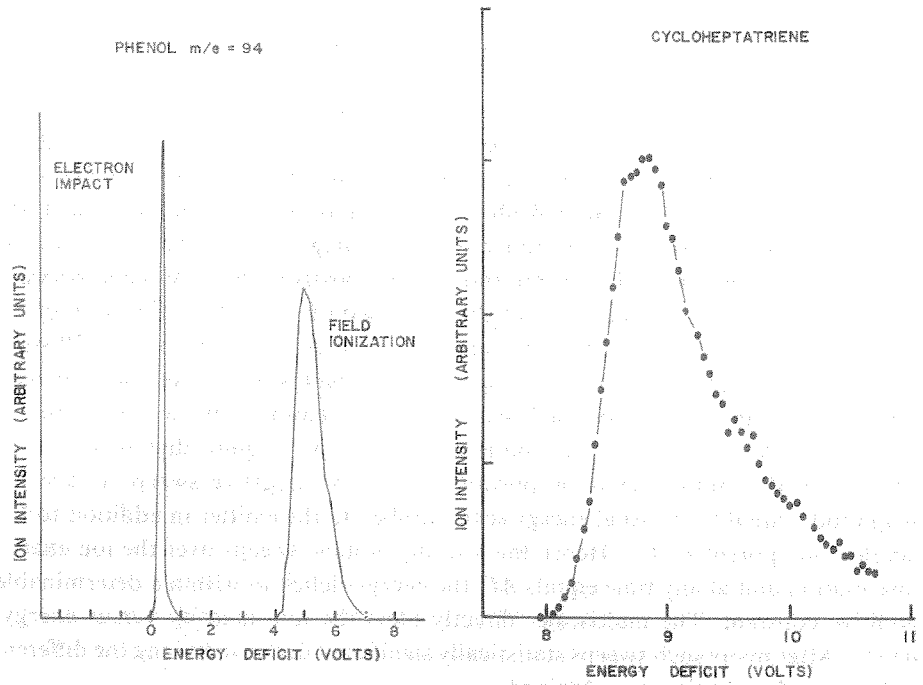

Fig. 2. (left) A plot of the parent ion intensity for phenol on the ordinate and energy-deficit in volts on the abscissa. The electron bombardment peak was obtained using a conventional electron bombardment source with an accelerating potential of V_0. The same potential was then applied to the field ion emitter and the phenol peak appears at an energy-deficit of ca. 4.2 V.

Fig. 3. (right) Field ionization energy spectrum of toluene. Ion intensity is plotted on the ordinate in arbitrary units and energy-deficit in volts on the abscissa. The energy-deficit scale has been adjusted by the quantity ϕ so that the critical energy-deficit numerically equals the ionization potential in electron volts.

right. The field ionization signal was then turned off and the electron beam source activated. Maintaining constant magnetic field and applying the same accelerating and sweep potentials to the electron source, data were again accumulated by sweeps over the energy-deficit. This produced the peak on the left. The measurement of onset separations in this plot (ca. 4.2 V) is not strictly a measurement of critical energy-deficit, ΔE_c, because of small effects due to repeller and drawout potentials (ca. 0.1 V) encountered in the electron beam source. This uncertainty can be overcome best by use of retarding techniques which calibrate the energy-deficit scale to within the additive instrumental quantity φ as discussed previously.

Figure 3 gives the energy distribution for toluene on an expanded energy scale. The energy scale has been set so that the observed critical onset in volts numerically equals the accepted ionization potential, 8.82 eV [16, 17]. The peak rises to its maximum value in ca. 0.6 V from onset and subsides into a long tail. The width of the peak is ca. 1 V at half-maximum, considerably broader than the

instrumental resolution which for these cases is ca. 200 mV. The width is attributed to a combination of: (1) "inherent" width arising from factors involving the surface structure of the tip and tunneling probability, and (2) width due to the involvement of excited ionic states in the field ionization process. We believe that much of the structure in the distribution arises from this latter effect.

The separation of these two effects can be accomplished by obtaining a sufficient quantity of data on the energy spectra of many molecular systems. Those features common to all spectra are due to "pure" surface effects while structure which correlates with molecular energy levels is a separable function of the molecule under investigation. Many of the energy distribution details are probably not separable into these two effects but depend on both molecular and surface structure. Other effects such as metastable broadening of the distributions and partial supply of a species through a surface reaction may arise because of the unique geometry of field ionization. These additional complexities may be of advantage for particular applications and form part of the utility and interest of the field ionization process.

The data in Fig. 3 show definite structure which is different for toluene than for other molecules. High-resolution photoionization data for toluene show a gradual onset with several resolved "steps". These features correspond well with the structure perceptible in Fig. 3. Such structure is reproducible in repeated runs as long as instrumental stability is not taxed by excessive data accumulation times. The statistical error in spectra intensity (as calculated by the square-root of the peak number of ion counts) is ca. 3 %.

Figure 4 shows the field ionization spectrum of cycloheptatriene with onset at the appropriate appearance potential (8.28 V) [17]. The distribution rises more rapidly from background with increasing energy-deficit than does that of toluene. Additionally the shape of the curve is different from that of toluene. The differences noted in the energy-deficit spectra are in general accord with the differences noted in the photoionization studies of these molecules. The structure in the photoionization cross-section is attributed to transitions to excited electronic–vibrational states of the molecular ion. With this view we suggest the structure in the field ionization energy-deficit spectra reflects the energy structure of the molecular ion and the relative transition probabilities. The resolution of the field ionization results is less than the photoionization results and hence the effects of rotational and vibrational excitation are not easily resolved. Consequently a detailed assignment or discussion is not at this time realizable. Similar considerations apply to Fig. 5 which shows the field ionization energy spectrum of phenol. In particular photoelectron data [18] show an electronic state 0.7 eV above onset. This correlates with a corresponding unresolved structure at ca. 10 V in Fig. 5.

The data presented for the three organic molecules show structure which is only partially resolved and difficult to interpret in terms of molecular structure. It should be noted, however, that the three distributions differ from one another

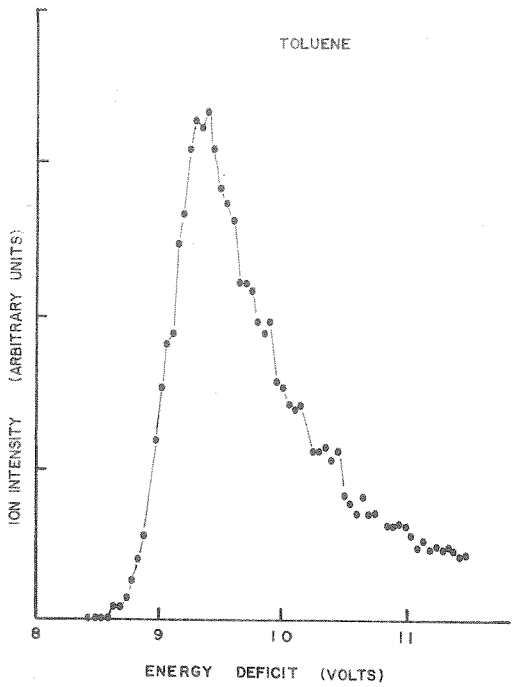

Fig. 4. Field ionization energy spectrum of cycloheptatriene. Ion intensity is plotted on the ordinate in arbitrary units and energy-deficit in volts on the abscissa. The energy-deficit scale has been adjusted by the quantity ϕ so that the critical energy-deficit numerically equals the ionization potential in electron volts.

in ways consistent with the differences in molecular energy structures. Our main point has been that upper states of ions produced by field ionization contribute to the total ionization probability. Clearer examples of this are given by data for smaller molecules which involve well separated upper states. Figure 6 shows energy distributions obtained from the field ionization of hydrogen and carbon monoxide. The upper two plots show the energy spectra of the H_2^+ and H^+ ions, respectively, produced by field ionization of molecular hydrogen. Here the energy-deficit has been shifted by addition of the quantity φ so that the distribution-onset coincides with the ionization potential. The high energy-deficit structure in the H_2^+ spectrum has been studied and interpreted previously [6, 12] and is not related to upper states of the ion. The pertinent portion of this plot occurs in the main peak with onset energy-deficit of ca. 15 V. This represents ionization through a transition from the ground state of the neutral molecule to the ground electronic and first few vibrational states of the ion. The effect of rotational excitation of the ion is ignored; rotational levels have small separations. In general, individual rotational levels are not resolved in the energy spectra although they may cause broadening of distribution structure. This effect may be particularly observable

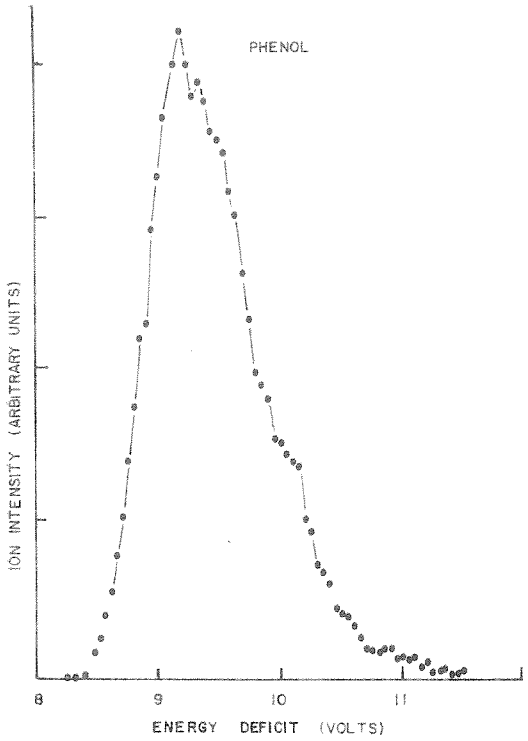

Fig. 5. Field ionization energy spectrum of phenol. Ion intensity is plotted on the ordinate in arbitrary units and energy-deficit in volts on the abscissa. The energy-deficit scale has been adjusted by the quantity ϕ so that the critical energy-deficit numerically equals the ionization potential in electron volts.

in the case of thermal excitation to levels of high multiplicity (so-called "hot bands") as ions with energy less than ΔE_c in the form of low-deficit tailing or resolved structure. However, as shown by Hanson [14], ionic rotation may have strong influence on dissociation probabilities. Excited neutral states of an inert gas have also been observed below the critical energy-deficit and interpreted as arising from bombardment of atoms near the surface by the electrons from atoms which have just ionized [19].

The molecular potential energy curves for neutral and singly ionized hydrogen and carbon monoxide shown in Fig. 7 are helpful in understanding the data of Fig. 6. In Fig. 7 the solid lines are the molecular curves with no applied electric field. It has been shown that upon application of a field no first-order effect is present for the neutral molecule. The ionic curves, however, are "distorted" by the addition of an effect proportional to the field and dependent on the mass and charge of the ion fragments at large internuclear separation. Specifically this term for large R, the internuclear separation, is $-\{eM_1/(M_1+M_2)\}FR$ for a

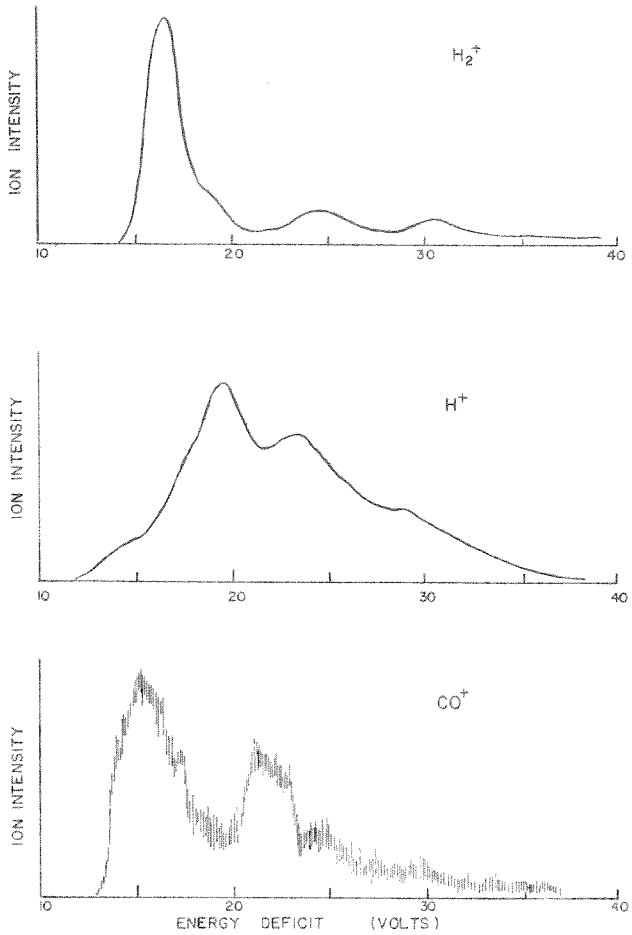

Fig. 6. Field ionization energy spectra of hydrogen and carbon monoxide. Ion intensity is plotted in arbitrary units on the ordinate and energy-deficit in volts on the abscissa. The energy-deficit scales have been adjusted by the quantity ϕ so that the critical energy-deficits numerically equal the ionization potentials in electron volts. Upper: the parent ion, H_2^+, from H_2 in field ionization; center: the dissociation fragment H^+ from the field ionization of H_2; lower: the parent ion CO^+ from the field ionization of CO.

singly charged ion oriented along the field [20]. Here M_1 is the mass of the charged fragment displaced from the center of mass along the field and M_2 the neutral fragment displaced against the field. This term has been added to the unperturbed ion ground state curves in Fig. 7 using the appropriate experimental value of F to produce the dashed curves.

The transition which produced the main peak in the upper plot of Fig. 6 is indicated as transition A in Fig. 7(a). Transitions to ionic vibrational states higher

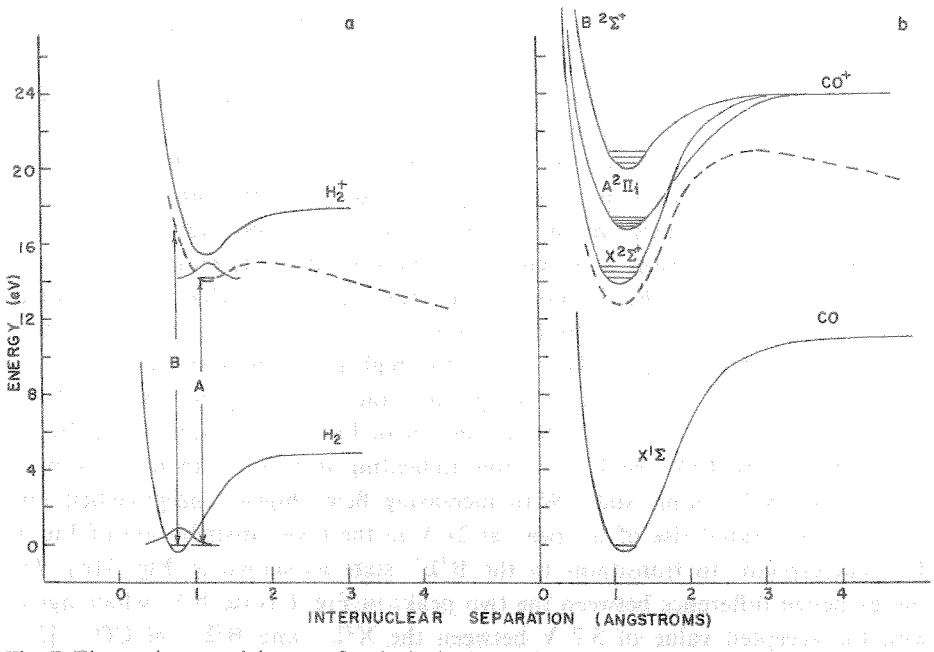

Fig. 7. Electronic potential curves for the hydrogen and carbon monoxide systems. The ordinate is electronic energy in eV and the abscissa is internuclear distance in Å. (a) Consideration of the potential curves for hydrogen show two types of transition which are observed. The transitions labeled A go from the ground state of the neutral to a bound vibrational level of the field-distorted molecular ion curve. Since the dissociation energy of H_2^+ is small the field distortion of the H_2^+ curve makes dissociative transitions (labeled B) possible at energy-deficits slightly above the H_2^+ onset. (b) Presumed potential energy curves for CO and CO^+ showing the three electronic states of CO^+ observed in optical spectra and which are presumably observed in the field ionization spectra. The behavior of the CO^+ curves at large internuclear separation are not known and are assumed to arise from the same separated atom states by comparison with the behavior of N_2^+ which is isoelectronic to CO^+. A field-distorted curve for the lower ionic state is also given.

than the first few states lead to dissociation arising from distortion of the ion energy curve by the high electric field (ca. 2.7 V $Å^{-1}$ in this example) as shown by transition B in Fig. 7(a). Taking into account the energy necessary for this transition and the subsequent motion of the ion fragments, the energy spectrum for H^+ (center spectrum Fig. 6) is explainable [14].

These considerations also explain the mass spectrum of H_2 as a function of electric field. At low fields (below about 2 V A^{-1}) only a narrow H_2^+ peak is observed; only the lowest energy transitions have appreciable probability. As the field is increased the dashed curve in Fig. 7a is further distorted as discussed above with consequent decrease in the number of bound ionic states. However, the main effect is to increase the probability of transitions to higher levels with consequent dissociation and hence appearance of ions at high energy deficit. The H^+ distribution at threshold fields is narrow, again, because transitions leading

to higher energy deficit ions have low probability. This distribution broadens rapidly with increasing field and dominates the mass spectrum. The pertinent points to observe in the first two plots of Fig. 6 are the two physically distinguishable transitions, from the ground state to bound H_2^+ and to dissociated $H+H^+$. The two modes belong to the same electronic state, and differ only in total energy. The energy deficit of each peak is ordered according to state energy. However, because of kinetic considerations the dissociation peak position is not simply given by adding the dissociation energy to the ionization potential [13, 14].

The lower plot in Fig. 6 shows the energy spectrum of CO^+ ions produced by field ionization of a CO sample. No dissociation is observed during the field ionization of CO principally because of the high ionic dissociation energy and the close alignment of minima in the ground-state molecular curves of CO and CO^+ with internuclear coordinates as shown in Fig. 7(b). Similar to hydrogen at low fields, the CO^+ peak is narrow indicating transitions from the ground state to the $X^2\Sigma^+$ ionic state. With increasing fields higher energy-deficit ions appear with a rapid rise of the peak at 21 V in the lower distribution of Fig. 6. This corresponds to transitions to the $B^2\Sigma^+$ state as shown in Fig. 7(b). The energy-deficit difference between the two peaks in Fig. 6 is ca. 6 V, which agrees with the accepted value of 5.7 V between the $X^2\Sigma^+$ and $B^2\Sigma^+$ of CO^+ [21]. Transitions to the $A^2\Pi_i$ state should be possible and may form the partially resolved structure in the low energy–deficit peak apparent at ca. 17 V in the CO^+ curve of Fig. 6. This state is expected to appear at an energy–deficit of 16.7 V using accepted values of its energy [21]. The peaks in the CO^+ distribution are relatively broad, implying transitions to a series of vibrational–rotational states belonging to one of the three electronic states of CO^+ shown in the diagram. The oscillator strengths of CO^+ implied by the field ionization data of Fig. 6 compare well with photoionization yield data [22]. The method of this comparison is not, however, well defined since the factor relating ionization probability per unit oscillator strength as a function of energy–deficit for a given electric field and tip surface configuration is not known. Furthermore, the contribution of auto-ionization to field ionization has not been explicitly determined so that it is not known whether deconvolution of autoionization contributions from the photo-ionization yield should be attempted for proper comparison.

In discussing field ionization, we have made the assumption of "vertical transitions" – as have other workers in this field. This assumption of the validity of the Franck–Condon principle for field ionization has been justified on the basis that ionization occurs very rapidly as compared with the period of molecular vibration. However, since the Franck–Condon principle rests on the Born–Oppenheimer approximation this viewpoint should be justified by experiment or theoretical examination of the validity of the Born-Oppenheimer separation of the molecular Hamiltonian with the addition of field dependent terms. Experimental results, however, are consistent with the hypothesis that the Franck–Condon

principle is obeyed to first order. This might be expected on a theoretical basis simply because the matrix element connecting neutral and ionic states is to first order given by a dipole term; the perturbing potential is eFx where F is the field, e the charge on the electron and x the nucleus-electron separation. On this basis the transitions should obey optical selection rules and have similar relative oscillator strengths.

We have not presented results for the dependence of the spectra on electric field. Qualitative conclusions for the H_2^+ and CO^+ spectra do not change appreciably with field; portions of the spectra change in relative intensity owing mainly to the variation of relative ionization probability and material supply [23] to different spatial regions. The spectra of the three organic molecules discussed differ very little with fields increasing from threshold until a sharp increase in the high energy–deficit tail is noted with consequent broadening of the distribution and decrease in intensity of the main peak near ΔE_c. The term "high energy–deficit" as used here is defined in terms of spatial location by more quantitative considerations in ref. 23. The details of the high energy–deficit tail were not examined for instrumental reasons but will form a topic for future investigation. The increase in the high energy–deficit portion of the spectrum can be interpreted in two ways: (1) An increase in ionization occurring at distances far from the tip and to the same final molecular states as at low fields, and (2) an increase in the probability of transition to excited ionic states. In either case, when dissociation is not involved, for a given energy–deficit, ionization occurs at the same spatial location Hence the final state energy of the electron which has tunneled into the metal is the same for both cases. First-order tunneling considerations (i.e. the WKB approximation) then directly give a ratio of transition rates for (1) to (2) which is independent of field. However, such a calculation neglects certain critical features of the problem. Among these are the relative symmetries of the final and initial states and the density of electronic states in the metal. Hence the ratio of rates for processes (1) and (2) may vary with molecular species and specific surface location.

It is to be noted that the rate of a particular type of reaction varies strongly with reaction energy as well as field. For example, the field necessary to produce a given ionization probability varies as the 3/2 power of the ionization potential [23]. Hence the field required for ionization of the organic molecules is less than for hydrogen and carbon monoxide.

CONCLUSIONS

Involvement of excited ionic states in field ionization is substantiated by experimental energy spectra and hence are to be considered in assessing the rate of any field ionization reaction. The amount of internal energy in the field-ionized molecule is determined by the particular structure of the molecule, the electric

field and the structure of the emitter surface. The energy spectrum of CO^+ shows clear and direct evidence of transitions to non-dissociative excited ionic states. Data for the organic molecules studied have not shown clearly resolved states although the energy spectra differ with molecular structure and are consistent with photon bombardment results.

At threshold fields the rate of ionization is appreciable only for transitions to the ground electronic state and lowest vibration–rotation states. As the field is increased the involvement of higher states remains small until the field is large enough to allow high energy–deficit transitions to become likely. The high energy–deficit ionization is seen to involve transitions to excited ionic states. Further theoretical and experimental work is needed to understand the selection rules and rates for transitions to excited states. In particular, the transition to dissociative states is of importance but is more complex than non-dissociative transitions and has not been extensively discussed here.

The fact that the energy of a transition is manifested in the energy spectra admits the possibility of distinguishing between transitions by measurement of ion energies. This has potential application to the interpretation of field ionization mass spectra in that distinctions may be made between reactions involving transitions to differing energies by this technique. An example of this has been given. The two mass isomers, toluene and cycloheptatriene, are distinguishable by differing onset energies and distribution shapes. At low fields dissociation-onset energy–deficits are larger than parent-onsets although may not be simply related to the dissociation energy. In general, however, the ordering of state energies is preserved in the spectra. Ions produced by surface reactions also have characteristic onsets which are related to formation energies; a common example of this is the protonation reaction seen in field ion mass spectra. The energy spectrum of the simplest protonation reaction, trimer formation from hydrogen or deuterium samples, is shown in ref. 6 where the trimer is distinguishable from a mass isomer. Metastable ions are commonly identified by energy analysis. These ideas may be implemented in practice by the addition of a retarding energy analyzer to the field ionization source of a mass spectrometer. A type of analyzer suitable for this application is described in ref. 6.

REFERENCES

1 E. W. Müller and T. T. Tsong, *Field Ion Microscopy: Principles and Applications*, American Elsevier Publishing Corp., New York, 1969. This book reviews the method and applications of the field ionization technique which were to a great extent developed in the senior author's laboratory over a period of several decades.

2 H. D. Beckey, *Field Ionization Mass Spectrometry*, Pergamon, New York, 1971. This book details and summarizes the author's contributions to mass spectrometry utilizing the field ionization technique.

3 This relationship has been given by many authors. See, for example, R. Gomer, *Field Emission and Field Ionization*, Harvard University Press, Cambridge, Mass., 1961. Also see refs. 1 and 2.
4 I. V. Goldenfeld, I. Z. Korostyshevsky and B. G. Mischunchuk, *Int. J. Mass Spectrom. Ion Phys.*, 13 (1974) 297.
5 T. T. Tsong and E. W. Müller, *J. Chem. Phys.*, 41 (1964) 3279.
6 A. J. Jason, *Phys. Rev.*, 156 (2) (1967) 266.
7 M. G. Inghram and R. Gomer, *Z. Naturforsch. A*, 10 (1955) 869.
8 M. G. Inghram and R. J. Gomer, *J. Chem. Phys.*, 22 (1954) 1279.
9 R. D. Young and E. W. Müller, *Phys. Rev.*, 113 (1959) 115.
10 E. W. Müller and K. Bahadur, *Phys. Rev.*, 99 (1955) 1651.
11 E. W. Müller and K. Bahadur, *Phys. Rev.*, 102 (1956) 624.
12 A. J. Jason, R. P. Burns and M. G. Inghram, *J. Chem. Phys.*, 43 (1965) 3762.
13 G. R. Hanson, G. E. Humes and M. G. Inghram, *Chem. Phys. Lett.*, 27 (1974) 479.
14 G. R. Hanson, *J. Chem. Phys.*, 62 (1975) 1161.
15 C. F. Giese, *Rev. Sci. Instrum.*, 30 (1959) 260.
16 J. L. Franklin et al., *Ionization Potential, Appearance Potential and Heats of Formation of Gaseous Positive Ions*, NSRDS-NBS-76, Superintendent of Documents, U.S. Government Printing Office, Washington, D.C.
17 F. A. Elder, Ph.D. Thesis, Department of Chemistry, University of Chicago, 1968.
18 A. D. Baker, D. P. May and D. W. Turner, *J. Chem. Soc. B*, 1968 (1968) 22.
19 E. W. Müller and S. V. Krishnaswamy, *Surface Sci.*, 36 (1973) 29.
20 J. R. Hiskes, *Phys. Rev.*, 122 (1961) 1207.
21 Gerhard Herzberg, *Molecular Spectra and Molecular Structure I. Spectra of Diatomic Molecules*, Van Nostrand, Princeton, N.J., 1950.
22 G. R. Cook, D. H. Metzger and M. Ogawa, *Can. J. Phys.*, 43 (1965) 1706.
23 A. J. Jason, A. C. Parr and M. G. Inghram, *Phys. Rev., B*, 7 (1973) 2883.